THE RATE OF EXCHANGE OF TRITIATED WATER ACROSS THE HUMAN RED CELL MEMBRANE*· ‡

By C. V. PAGANELLI§ AND A. K. SOLOMON

(From the Biophysical Laboratory of Harvard Medical School, Boston)

(Received for publication, May 3, 1957)

ABSTRACT

The flow method of reaction rate measurement has been adapted to the determination of the rate of diffusion of water into the human red cell. In seven experiments the half-time for diffusion exchange has been found to be 4.2 ± 1.1 msec., which is equivalent to a diffusion flow of 8.6×10^{-9} ml. H_2O/(sec., red cell). This figure has been compared with the rate of water entrance under an osmotic pressure gradient, and has been found to be smaller by a factor of 2.5. The difference between these two rates of water entrance has been interpreted as indicating the presence of water-filled channels in the membrane. An estimate of the equivalent radius of these channels (on the assumption of uniform right cylindrical pores) leads to a value of 3.5 Å, which is viewed as an operational description of the resistance offered by the membrane to the passage of water.

The present experiments were undertaken to measure the *in vitro* exchange rate of water across the human red cell membrane under isotonic conditions, using tritiated water (THO) as a tracer. To determine the time course of this rapid exchange, a flow method was devised, based on the principles developed by Hartridge and Roughton (1), Dirken and Mook (2), and Chance (3). Freshly drawn, heparinized, whole blood or fresh red cell suspensions were mixed with an isotonic red cell buffer containing THO, and the rate of uptake of the THO by the cells was followed. The rates of entrance of water by diffusion and by osmosis were then used to calculate an equivalent pore size for the red cell membrane.

Experimental Method

Principles.—

A suspension of cells and tritiated, isotonic buffer is mixed and forced down an observation tube. As the mixture flows down the tube, the non-labelled intracellular

* This study was supported in part by the Atomic Energy Commission.

‡ A preliminary report appeared in *Fed. Proc.*, 1956, **15**, 140.

§ The support of a National Institutes of Health predoctoral fellowship administered by the National Heart Institute, is gratefully acknowledged.

water and the labelled extracellular water start to exchange. The extracellular water is sampled at intervals along the tube through filters which red cells cannot pass. The samples of labelled filtrate, each representing a certain time of exchange, are analyzed for their tritium content, and a kinetic curve, showing the fall in concentration of labelled water as a function of time, is plotted. A schematic diagram of the flow system is shown in Fig. 1.

Details of Construction.—

(*a*) *Reagent Containers.*—The reagent containers are 1500 ml. stainless steel beakers fitted with tops made of ¼ inch brass plates. The plates are screwed down against No. 53 O-rings to form a pressure seal. A Hoke No. 306 needle valve is fitted to one plate and serves as a pressure release. No. 6 gauge stainless steel tubing (0.203

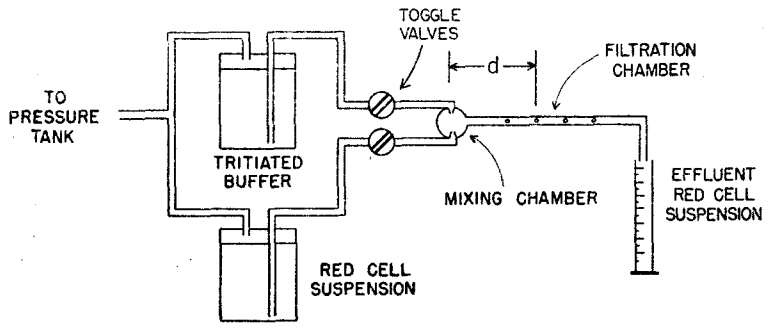

FIG. 1. Schematic drawing showing flow system. Gas under pressure forces the tritiated buffer and the red cell suspension through the open toggle valves into the mixing chamber. After mixing the fluid flows at a velocity of about 9.5 meters/sec. through the filtration chamber into the graduate where the effluent fluid is collected. Four samples are taken during flow through the filtration chamber.

inch outer diameter, 0.015 inch wall thickness) is hard soldered to the plates to form outlets for the flow solutions. ¼ inch copper tubing connects the tank of 95 per cent air, 5 per cent CO_2 to the beakers. Two pieces of vinyl tubing (⅛ inch inner diameter 1/32 inch wall thickness) which pass through the special toggle valves shown in detail in Fig. 2, connect the ends of the stainless steeel tubing to the jets of the mixing chamber.

(*b*) *Mixing Chamber.*—The mixing chamber, shown in Fig. 2, is machined from a ⅜ inch lucite sheet and all the machined surfaces are polished. Its dimensions are given in Fig. 2.

(*c*) *Filtration Chambers.*—Fig. 3 shows the design of the filtration chamber used in the present experiments. A piece of No. 12 gauge stainless steel tubing (0.085 inch inner diameter, 0.012 inch wall thickness) is imbedded lengthwise in a lucite block 3¼ inch × 1 inch × 5/16 inch. Four cylindrical surfaces of 1 1/32 inch radius are milled at 2 cm. intervals into the lucite and the wall of the tubing until the wall is very thin. Then four 1/16 inch holes are drilled through the tubing wall at the thin spots.

In this way, practically no dead space, in which stagnant fluid might accumulate, is left between the filters and the flowing solutions. Seven mm. circles of Millipore filter paper (0.8 μ pore diameter, Aerosol Assay, Millipore Filter Corporation, Waltham, Massachusetts), backed by circles of ordinary filter paper (Whatman No. 42) for mechanical strength, are placed in position over the holes of the tube. They are held down tightly by segments of cylinders of $1\frac{1}{32}$ inch radius, which are bolted to the lucite block, as shown in Fig. 3. Holes in the segments permit passage of fluid through the filters. With this arrangement, four samples can be filtered simultaneously, and thus a single experiment provides sufficient data for four points on a

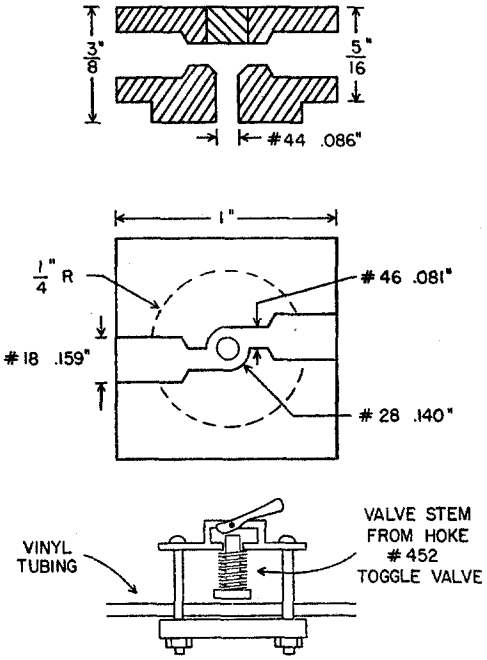

FIG. 2. Top, side view of mixing chamber. Center, top view of mixing chamber. Bottom, detail showing toggle valve.

kinetic curve. The filtration chamber produces a total of about 0.1 ml. filtrate from 500 ml. of reactants.

(*d*) *Sampling Pipettes.*—The filtration chamber is fastened to the mixing chamber hole-side downward in normal use, and four capillary pipettes are placed with their tips close to the holes. Thus as fluid is filtered, it is drawn into the pipettes by capillary attraction. The pipettes are mounted on the stage of a misco rack-and-pinion micromanipulator to facilitate their positioning.

Experimental Procedure.—

Three basic types of flow experiments were performed: (1) whole, heparinized blood (sodium heparin, Lederle, 10 mg./ml.; 0.5 ml. added to 100 ml. blood) was

allowed to exchange with an 0.9 per cent solution of NaCl made up with THO. (2) 500 ml. of whole, heparinized blood were centrifuged for one-half hour at 890 *g*, and the bulk of the plasma was removed. The "packed" cells (hematocrit reading around 0.8) were allowed to exchange with their own plasma to which about 0.1 ml. of THO of high specific activity had been added. (3) 500 ml. of whole, heparinized blood were centrifuged for one-half hour at 890 *g*, and about 200 ml. of plasma were removed. The plasma was replaced with 100 ml. of an isotonic phosphate-bicarbonate buffer whose composition is given in Reference 4, Table I. This enriched cell suspension (hematocrit reading about 0.6) was allowed to exchange with the same phosphate-bicarbonate buffer made up with THO.

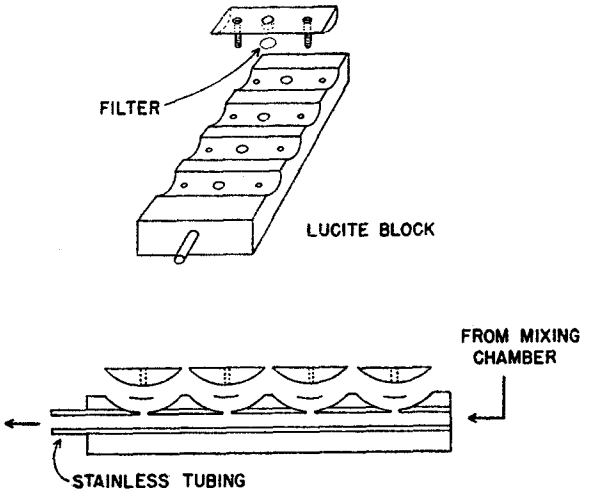

FIG. 3. Detail showing filtration chamber.

Tritium Measurement.—

The THO in the filtrates was diluted by weight and assayed by the methane, proportional counting method of Robinson (5). The reproducibility of this method was checked by assaying a single sample of THO eight times. The results agreed to a standard deviation of ±0.7 per cent.

RESULTS

Performance of Equipment

(*a*) *Efficiency of Mixing.*—The efficiency of the mixing chamber was tested by using human red cells labelled with $Cr^{51}O_4^{=}$ (obtained from Abbott Laboratories, North Chicago, Illinois, as a solution of $Na_2Cr^{51}O_4$). A suspension of the labelled cells (hematocrit reading about 0.4) in 0.9 per cent NaCl was placed in one of the steel beakers of the flow system, and a solution of 0.9 per cent NaCl was placed in the other beaker. A 10 ml. hypodermic syringe barrel carrying a 26 gauge needle was mounted on a misco micromanipulator, and

the needle was inserted into the observation tube. Then the cell suspension and the NaCl solution were forced into the mixer and down the observation tube at 814 cm./sec. A sample of the mixture flowing down the tube was taken by applying a vacuum to the syringe barrel. In three separate experiments, samples were taken at the rear wall of the mixing chamber itself, at the orifice of the mixing chamber, and 1.6 mm. from the orifice. The cell suspension flowing from the end of the observation tube was also collected in each of the three experiments, and thoroughly mixed by shaking. The specific activities of the collected cell suspensions were determined in a well-type scintillation counter. The Cr^{51} concentration in the effluent suspension was used to represent 100 per

TABLE I

Efficiency of Mixing

Position of sampling	Time	Mixing
	msec.	*per cent*
Back wall of mixing chamber	~0	78.2
Orifice of mixing chamber	0.67	82.3
1.6 mm. from orifice of mixing chamber	0.87	97.5

cent mixing, and the percentage mixing at each sampling position in the observation tube was calculated as

$$100 \times \frac{Cr^{51} \text{ concentration, sample}}{Cr^{51} \text{ concentration, effluent}}$$

Table I shows the results of these experiments. It will be seen that mixing is at least 97.5 per cent complete in about 0.9 msec.

The time spent by the fluid in the mixing chamber must be taken into account in computation of reaction times of the four filtered samples. For this purpose, the formula of Hartridge and Roughton (1) for the equivalent length of the mixing chamber was used:

$$L_0 = r_m^2 L_m / r_0^2 \tag{1}$$

in which L_0 is the equivalent length of the mixing chamber in cm., r_m is the radius of the mixing chamber (cm.), r_0 is the radius of the observation tube (cm.), and L_m is the length of the mixing chamber (cm.). L_0 for the mixing chamber shown in Fig. 2 is 0.54 cm. This distance was added to the distance from the mixing chamber to each of the four points of filtration when reaction times were calculated.

(*b*) *Nature of Flow in the Filtration Chamber.*—The critical velocity for turbulent flow in the filtration chamber was calculated from the Reynolds formula:

$$\mu_c = 1000\eta / \rho r_0 \tag{2}$$

in which μ_c is the critical velocity in cm./sec., η is the viscosity in poises, and ρ is the density in gm./cm.^{3}. Coulter and Pappenheimer (6) have shown the validity of this equation for bovine blood at many different hematocrit readings. The following approximate values were used: $\eta = 0.07$ poise (the apparent viscosity of bovine blood just below turbulence; hematocrit reading = 0.53, temperature = 28°C. (6)); $r_0 = 0.109$ cm., and $\rho = 1.0$ gm./cm.^{3} With these values, $\mu_c = 640$ cm./sec. In practice, this velocity was always exceeded by at least 200 cm./sec., so that flow in the filtration chamber was always turbulent.

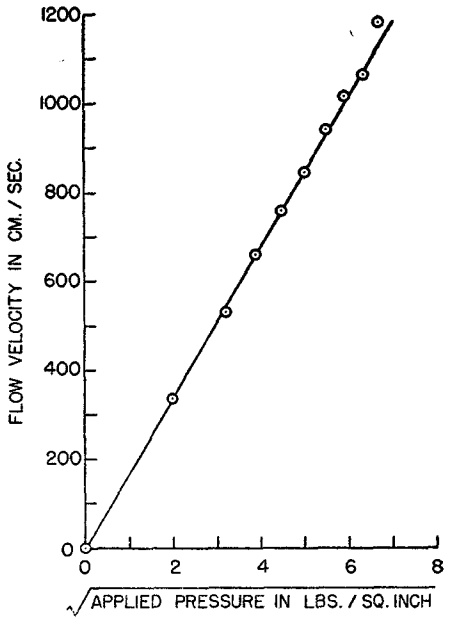

FIG. 4. Pressure-flow curve for mixing chamber and observation tube.

In addition, a pressure-flow diagram was plotted for the filtration chamber. The linear relation between flow rate and the square root of the pressure shown in Fig. 4 is typical of the turbulent flow; it would not have been obtained had there been laminar flow in the filtration chamber, which is characterized by a linear relation between flow and pressure.

The steadiness of the flow rate was checked by repeated measurement of the volume outflow per unit time. In six trials, each lasting 6.0 sec., the volume outflow was constant to within a standard deviation of ± 2.4 per cent.

(*c*) *Memory Effects.*—To prevent memory effects caused by residual radioactivity, the entire flow system was repeatedly rinsed in distilled water after each experiment. The parts of the system which were not plastic were dried at 100°C. The plastic parts (mixing chamber and filtration chamber) were

dried in an air stream. The sampling pipettes, which were made from pyrex capillary tubing, were discarded after each experiment. These measures were sufficient to insure the absence of any appreciable memory.

Hemolysis and Net Water Movement in Red Cells

The degree of hemolysis of the effluent cell suspension was determined as routine in preliminary experiments with the flow system. Hemoglobin concentration, as measured on a Beckman model B spectrophotometer at 4160 Å, was used as the measure of hemolysis. In five preliminary experiments, the degree of hemolysis averaged 0.3 per cent; accordingly, routine hemolysis measurements were discontinued after Experiment 7. Visual estimation of the color of the red cell suspension medium after an experiment served to guard against gross hemolysis.

TABLE II

Changes in Relative Mean Corpuscular Hemoglobin Content (mchc)

Experiment No.	Relative mchc (Relative Hb content/volume of cells)		Difference
	Before experiment	After experiment	
			per cent
8	2.03	2.34	+15.2
9	2.13	2.11	−0.9
10	2.06	2.11	+2.4
11	2.03	1.99	−2.0
12	1.85	1.92	+3.8
13	2.04	2.15	+5.4

Relative mean corpuscular hemoglobin concentration (mchc) determinations were made before and after each experiment as a check on the constancy of cell water content. The determination depended on hemoglobin analysis by the method outlined above, and hematocrit readings in standard Wintrobe tubes spun at 1610 *g* for 50 minutes. Table II shows the changes in relative mchc which took place in the course of six experiments. These changes reflect water shifts occurring in the red cell; a positive change indicates cell shrinkage, and a negative change, cell swelling. A relatively large water movement was observed in Experiment 8, but in the remaining five experiments, the water shifts were small and of doubtful significance in view of the 1.9 per cent standard deviation in the hemoglobin determinations (7).

Mathematical Treatment of Data

The equations to be presented describe the diffusion of tritiated water across the red cell membrane, subject to certain assumptions: (a) the cell interior and

the suspension medium behave as two well mixed compartments; (b) the cells neither gain nor lose water during a diffusion experiment; (c) tritiated water acts as an ideal tracer for ordinary water; (d) the radiation of the tritium molecules does not disturb normal cell processes. Under these conditions, the following equations may be used to describe the water exchange (8):

$$\frac{dP}{dt} = -kp + kq \tag{3}$$

$$P = pv_p \tag{4}$$

$$p_0v_p = pv_p + qv_q \tag{5}$$

In these equations, P is the amount of THO present in the suspension medium, t is time, k is a proportionality constant, p and q are the specific activities of the water of the suspension medium and the cell interior, respectively, v_p and v_q are the volumes of the suspension medium and the intracellular water, respectively, and p_0 is the value of p at $t = 0$. The assumptions given above require discussion and qualification to show that they are satisfied reasonably well in these experiments.

(*a*) *Assumption of Two Well Mixed Compartments.*—The first assumption, as applied to the suspension medium, is subject to experimental proof. The evidence given in Table I shows the suspension medium to be well mixed, at least at 0.87 msec. after the reaction is initiated. The degree of mixing in the cell interior cannot be verified experimentally, but it is possible to calculate how rapidly diffusion alone would produce a given degree of mixing in the interior. Roughton's (9) treatment of the diffusion of dissolved oxygen in the red cell interior has been adapted for this purpose. In this treatment, the red cell is considered as a plane liquid sheet. It is possible to show that a substance present on both sides of such a sheet diffuses into the sheet according to the equation:

$$\frac{\bar{p}}{\bar{p}_0} = 1 - \frac{8}{\pi^2} e^{-(D\pi^2/4b^2)t} \tag{6}$$

in which $\bar{p}$ is the average specific activity of THO in the cell interior, $\bar{p}_0$ is the initial specific activity of THO outside the cell, D is the diffusion coefficient of THO in the cell interior, b is the half-thickness at the center of the red cell, and t is time. A value of D is necessary to calculate the time required for the cell interior to reach a concentration which is 90 per cent of $\bar{p}_0$. D is unknown, but may be estimated from the work of Wang (10) on the diffusion of H_2O^{18} into concentrated ovalbumin solutions. In a solution which was 24.5 per cent protein by weight, $D_{H_2O^{18}}$ was found to equal 0.978×10^{-5} cm.^{2}/sec. at 10°C. By using this value as a rough estimate of D in Equation 6, and setting b equal to 0.5×10^{-4} cm. (11), one obtains $t = 0.2$ msec. Thus, if no other force acts to mix the cell interior, diffusion alone produces mixing which is 90 per cent complete in about 0.2 msec. In these experiments the half-time for water exchange across the membrane is found to be about 4 msec. Thus the assumption of a well mixed cell compartment seems to be justified.

(*b*) *Steady-State Assumption.*—The second assumption, that the cells neither gain nor lose water during an experiment, has been tested experimentally, as already discussed. It is also possible to calculate the effect of osmotic shifts of water during the exchange of THO. Suppose that, because of anisotonicity of the tritiated buffer, or a shifting gas equilibrium, there is a 20 per cent difference in osmolarity between the cells and the buffer. When the cells and buffer are mixed, will the relatively large water shift induced by this difference in osmolarity occur rapidly enough to affect the kinetics of water exchange by diffusion? It is possible to answer this question by consideration of the rate at which water enters or leaves the red cell under an osmotic gradient. Sidel and Solomon (12) have estimated this rate as 1.5×10^{-14} ml. H_2O/(sec., cm. H_2O pressure, red cell) at 25°C. In 20 msec., therefore, with a 20 per cent difference in osmolarity, the red cell would gain or lose 5×10^{-13} ml. H_2O. This figure is less than 1 per cent of the red cell water volume. Since all the measurements of THO diffusion in the present study were done at times of 10 msec. or less, it is seen that osmotic water shifts can have little influence on these measurements.

(*c*) *Ideality of THO as a Tracer for H_2O.*—The third assumption, that THO acts as an ideal tracer for H_2O, is subject to some doubt. There is disagreement among different investigators as to the true values of the diffusion coefficients of THO, H_2O^{18}, and D_2O, and as to whether they may be used interchangeably as tracers for water in biological systems (13–17). For the purposes of these calculations, however, the data of Wang *et al.* (13) have been considered most satisfactory. They found the diffusion coefficient of THO to be 14 per cent smaller than that of H_2O^{18}, which is usually considered the most nearly ideal tracer for H_2O. Accordingly, H_2O fluxes, when calculated from measured THO fluxes, have been increased by 14 per cent to compensate for this difference.

(*d*) *Absence of Radiation Effects.*—The fourth assumption, that the radiation of the tritium molecules does not disturb normal cell processes, is subject to indirect experimental proof. Sheppard and Martin (18) showed that red cell suspensions subjected to 1200 r of γ radiation exhibited no change in their ability to transport potassium. In the present experiments, the radiation dosage was calculated to be less than 4×10^{-7} rad, an exposure which is minute in comparison with the 1200 r of Sheppard and Martin. Thus, the fourth assumption would seem to be valid.

(*e*) *Solution of the Diffusion Equation.*—To solve Equation 3, P and q are first eliminated by substitution from Equations 4 and 5. Using the boundary conditions $p = p_0$ when $t = 0$, and $p = p_\infty$ when $t = \infty$, the solution is:

$$\ln\left[\left(\frac{p}{p_\infty} - 1\right) \Big/ \left(\frac{p_0}{p_\infty} - 1\right)\right] = -\frac{k p_0 t}{v_q p_\infty} \tag{7}$$

or

$$\frac{p}{p_\infty} - 1 = \left(\frac{p_0}{p_\infty} - 1\right) e^{St} \tag{8}$$

in which $S = -kp_0/v_q p_\infty$. Fig. 5 shows a semilogarithmic graph of $(p/p_\infty - 1)$ against time for the data from a single experiment. The data plotted in this manner fall on a straight line, consistent with the postulated two-compartment kinetics. The rate constant k/v_q, which represents the fraction of red cell water exchanging in unit time, may be calculated from the slope S of this line. The half-time of the exchange may be obtained by setting $p = (p_0 + p_\infty)/2$, and $t = t_{1/2}$ in Equation 7. Thus, $t_{1/2} = -0.693/S$.

Experimental Determinations

The rate of exchange of THO across the human red cell under isotonic conditions was followed in seven samples of blood drawn from young adult males.

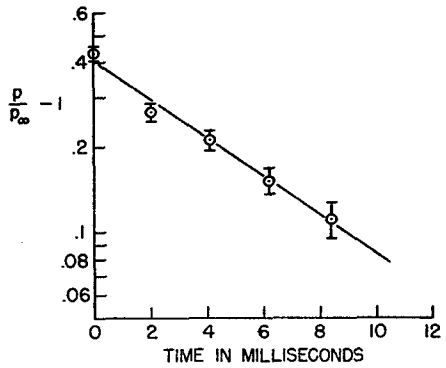

FIG. 5. THO uptake by human red cells in isotonic buffer. The points represent data from Experiment 13, with standard deviations, and the curve has been drawn as discussed in the text.

The half-time of the exchange was found to be 4.2 ± 1.1 msec. at 23°C. The half-time was independent of the hematocrit reading of the cell suspension over a twofold range, and independent of the nature of the suspension medium, as shown in Table III.

The data were treated mathematically according to the equations previously given. Taking 6.3×10^{-11} ml. as the average water content of the human red cell (19), and increasing the rate constant found for THO exchange by 14 per cent, as previously discussed, the unidirectional water flux is calculated to be 8.6×10^{-9} ml. H_2O/(sec., red cell).

Sources of Error

(*a*) *Errors of Experimental Design.*—Unless the two toggle valves which control the flow of tritiated buffer and cell suspension are opened simultaneously, the first portion of fluid to descend the observation tube will be richer in cells or in buffer than succeeding portions. This difference will be reflected

in the first drops of filtrate to be collected. If these first drops are discarded, the difference will be minimized. However, in view of the small amounts of filtrate usually collected (0.01 to 0.05 ml.), the residue of the first drops in the filtration chamber may be sufficient to contaminate the sample. If it were possible to take larger samples, the possibility of error from this source would be reduced.

The deceleration of flow which takes place until the entire outlet tube, from mixing chamber to graduated cylinder, has filled with solution, is another source of error. This deceleration has the effect of blurring the time axis along the observation tube until a steady flow has been established. Again, this

TABLE III

Summary of Data from Exchange Experiments

Experiment No.	Hematocrit reading		Suspension medium	Flow velocity	k/v_q	$t_{\frac{1}{2}}$
	Initial	Final				
				cm./sec.	*msec.*$^{-1}$	*msec.*
8	0.816	0.400	Plasma	845	0.146	3.0
9	0.461	0.258	0.9 per cent NaCl	925	0.155	3.5
11	0.455	0.251	PO_4–HCO_3 buffer*	958	0.138	3.9
12	0.629	0.512	PO_4–HCO_3 buffer + plasma	843	0.109	3.4
13	0.620	0.328	PO_4–HCO_3 buffer + plasma	937	0.111	4.4
14	0.591	0.322	PO_4–HCO_3 buffer + plasma	996	0.090	5.5
15	0.594	0.316	PO_4–HCO_3 buffer + plasma	925	0.082	5.9
Average					0.119	4.2
Standard deviation					±0.028	±1.1

* Buffer composition given in Reference 4.

error is minimized by discarding the filtrate until a steady flow has been established, but as in the previous case, small sample size creates an uncertainty.

The slit width error, caused by filtration of samples over a finite distance (the diameter of the holes in the filtration chamber), was calculated according to Equation 39 of Chance (3) and found to be much less than 1 per cent.

(*b*) *Errors in Measured Quantities.*—Errors in measured quantities are usually expressed as standard deviations of a set of replicate measurements. In some cases errors are estimated on the basis of smallest scale divisions. Such errors are marked with asterisks. However, all errors combined in the course of a calculation are treated as standard deviations for ease and uniformity of computation. The rules used for combination of error are to be found in Beers (20)

Linear Flow Velocity.—The error involved in calculation of linear flow velocity arises from three sources: error in timing, error in volume measurement,

and error in the bore of the observation tube. It is possible to measure the volume of effluent cell suspension to ±5 ml.* as it flows from the apparatus into the graduated cylinder. Since 350 ml. of suspension are usually collected, ±5 ml.* represents about ±1.4 per cent* error. Timing of the volume outflow of the system to ±0.002 minute, or ±1.3 per cent in a total of about 0.15 minute, is possible. Thus the volume rate of outflow is measured to ±2 per cent. The dimensions of the observation tube are given as 0.109 ± 0.001 inch outer diameter, 0.012 ± 0.001 inch wall thickness (manufacturer's specifications). The inner diameter calculated from these figures is 0.085 ± 0.002 inch or ±2.4 per cent. The cross-sectional area of the tube is calculated to be 0.0366 $cm.^2$ ± 4.8 per cent. The linear flow rate, computed from the volume flow rate and the cross-sectional area, is known to ±5.2 per cent.

Hematocrit Reading.—The error in hematocrit readings is taken as ±0.002,* or ±0.2 of the smallest scale division on an Exax "blue line" hematocrit tube. In general, duplicate hematocrit readings on the same blood agree to within ±0.002.

Dilution.—The filtrates are diluted by weight before being analyzed for their tritium contents. The standard deviation involved in weighing is found to be ±0.0001 gm., or ±1 per cent of the smallest quantity of filtrate used, in a set of ten replicates on the analytical balance used.

Counting.—The net counting rate is usually measured to a standard deviation of about ±1 per cent.

Reaction Time.—The error involved in calculating reaction times arises from two calculable errors, error in flow velocity (see above) and error in measurement of distance; and two incalculable errors, the estimates of the equivalent length of the mixing chamber, and the velocity profile of the flowing fluid. The distances along the observation tube were measured with a vernier caliper which was accurate to ±0.02* cm., or ±1.1 per cent in 1.85 cm., the shortest distance measured. Since the error in the flow velocity is ±5.2 per cent, its contribution to error in reaction time constitutes almost the entire calculable error.

Other Errors.—The incalculable errors pose a special problem. The first arises from the assumption, implicit in the application of Equation 1, that mixing is complete instantaneously. The results presented in Table I indicate that mixing is not complete at the back wall of the mixing chamber, and hence that Equation 1 is not quantitatively applicable. Alternately, Roughton (21) has suggested that the equivalent mixing length is given by "the product of t_m (the time for the mixing to be almost say 98 per cent, complete) and $\bar{u}$, the average of fluid flow in cm./sec." This latter estimate would lead to an equivalent mixing length of about 0.8 cm. in place of the value of 0.54 cm. calculated from Equation 1. The difference between these two figures is approximately equal to 0.25 msec. which lies well within the standard deviation of the final figure.

Furthermore, a delay of this magnitude would probably not introduce a measurable difference (inconsistency) in data such as that presented in Fig. 5.

The second error arises from the radial distribution of velocity of the fluid flowing down the observation tube.[1] Prandtl's equation, as quoted by Roughton (21), probably does not apply to an inhomogeneous suspension of cells and buffer flowing down an observation tube, with an appreciable centrifugal component of motion. The hydrodynamics of such a situation is most complex and no satisfactory theoretical solution is known to the authors. There must certainly be a stagnant layer of fluid present at the boundary between the moving fluid and the observation ports. If this boundary is as thin as a red cell, it should come to diffusion equilibrium so quickly that it will not contribute seriously to the over-all error of the method, as has been discussed above.

The arguments against the presence of a thick boundary layer, which will affect the results appreciably, are necessarily indirect. They are all based on the apparent consistency of the experimental data. The radial distribution of velocity in a turbulent rotating mass of cells in fluid would be expected to depend markedly on the relative density of cellular population. This is particularly so because the centrifugal component of force would tend to throw the cells out peripherally. The hematocrit reading of the suspensions used, as shown in Table III, varied over a twofold range, with the cells occupying, in some cases one-quarter, and in other cases up to one-half, of the volume of the flowing suspension. Nonetheless, the data show that the measured reaction rate is essentially independent of the hematocrit reading, and they support the conclusion that the boundary layer effect is unimportant in the present study.

Furthermore, the apparent half-time of the reaction is relatively independent of the velocity of flow over about a 15 per cent range. If any correlation exists, it appears that the slower rates of flow lead to faster reaction rates, a direction contrary to that expected if diffusion through a peripheral layer is the limiting factor. Finally, since the diffusion delay should be variable from sampling port to sampling port, it would not be expected that a curve of the kind exhibited in Fig. 5 would be obtained, except under the most fortuitous circumstances. It is concluded that the effect of radial velocity distribution, though undoubtedly present, is not important enough to become apparent over the other sources of error that have already been discussed in detail.

DISCUSSION

Comparison of Results with Water Diffusion Permeabilities of Other Cells and Membranes

Values of the water permeability constant (P_d) are given for a variety of biological membranes in Table IV. In each case, P_d was measured by the

[1] The authors would like to express their indebtedness to Dr. R. E. Forster for a stimulating discussion on this point.

diffusion of isotopic water. P_d for the human red cell is over 30 times the next largest value in the table, and nearly 250 times the smallest value. Thus the data from the present experiments are consistent with Jacobs' statement that the permeability of the erythrocyte to water "... is greater than that of any other known cell". (22)

Comparison with Filtation Permeability

It is instructive to compare the rates of water movement across the red cell membrane from diffusion and from osmotic flow The rate of water entrance under an osmotic gradient, determined by Sidel and Solomon (12), is 1.5 $\times$ 10^{-14} ml. H_2O/(sec., cm. H_2O pressure, red cell), as given previously. The rate of diffusion flow from the present experiments is 8.6×10^{-9} ml. H_2O/(sec., red cell). Since this rate was obtained from experiments in which the unidirectional flux of THO was measured, the concentration gradient for the diffusion of water was 55.2 moles/liter, which is equivalent to 1.38×10^6 cm. H_2O pressure at 23°C. Conversion of diffusion flow into units of osmotic flow gives $(8.6 \times 10^{-9})/(1.38 \times 10^6) = 0.62 \times 10^{-14}$ ml. H_2O/(sec., cm. H_2O pressure, red cell). Hence, osmotic flow is 2.5 times greater than diffusion flow. According to Ussing (29), a difference between the permeability constants for diffusion and filtration of water is indicative of the presence of water-filled channels in the membrane.

TABLE IV

Water Permeability Constants

Membrane	P_d	Temperature	Reference
	(*cm./sec.*) $\times 10^3$	°C.	
Human red cell	5.3	23	Present experiments
Amoeba (*Chaos chaos*)	0.0250	—	16
Amoeba proteus	0.021	20	23
Frog gastric mucosa	0.0483	25	24
Frog ovarian egg	0.128	—	25
Zebra fish ovarian egg	0.068	—	25
Xenopus body cavity egg	0.090	—	25
Zebra fish egg, shed, non-developing	0.036	—	25
Frog body cavity egg	0.075	—	25
Salmon egg, unactivated	0.168	—	26
Toad skin	0.113	22	27
Frog skin	0.073	—	28

Calculation of Equivalent Pore Size and Fractional Pore Area

A measure of the average size of these channels may be obtained by combining the two permeability constants according to the method given by Pappen-

heimer *et al.* (30), and Koefoed-Johnsen and Ussing (27). Let us consider an idealized membrane which contains an array of uniform, right-cylindrical pores. The diffusion of THO through these pores may be described by Fick's law, subject to certain assumptions which are discussed below.

$$\dot{q}_{THO} = -D_{THO} A_p \frac{\Delta C_{THO}}{\Delta x} \tag{9}$$

in which $\dot{q}_{THO}$ is the amount of THO crossing the membrane in moles/sec., D_{THO} is the diffusion coefficient of THO in the pores in cm.^{2}/sec., A_p is the total pore area of the membrane in cm.^{2}, ΔC_{THO} is the concentration difference of THO across the membrane in moles/cm.^{3}, and Δx is the length of the pores or the membrane thickness in cm. To convert the flow of THO to total water flow, it is necessary to assume that:

$$\frac{\dot{q}_{THO}}{\Delta C_{THO} D_{THO}} = \frac{\dot{q}_{H_2O}}{\Delta C_{H_2O} D_{H_2O}} \tag{10}$$

Then Equation 9 becomes:

$$\dot{q}_{H_2O} = -D_{H_2O} \left(\frac{A_p}{\Delta x}\right) \Delta C_{H_2O} \tag{11}$$

Multiplying both sides of Equation 11 by $\overline{V}_{H_2O}$, the partial molar volume of H_2O, converts flow in moles/sec. to $\dot{m}_{H_2O}$, the flow in ml./sec.:

$$\dot{q}_{H_2O}\overline{V}_{H_2O} = \dot{m}_{H_2O} = -D_{H_2O} \left(\frac{A_p}{\Delta x}\right) \overline{V}_{H_2O}\Delta C_{H_2O} \tag{12}$$

The term ΔC_{H_2O} represents the concentration difference for the unidirectional flux of water into the red cell. Since $\overline{V}_{H_2O} = 0.018$ liter H_2O/mole, and $\Delta C = 55.2$ moles/liter, the term $\overline{V}_{H_2O}\Delta C_{H_2O}$ is very close to unity. Equation 12 then becomes:

$$\dot{m}_{H_2O} \cong -D_{H_2O} \left(\frac{A_p}{\Delta x}\right) \tag{13}$$

Hence, from a measurement of diffusion flow and a knowledge of D_{H_2O}, one may calculate $A_p/\Delta x$, the pore area per unit path length in the membrane.

The next step in the calculation of equivalent pore size involves the use of Poiseuille's law, which describes the laminar flow of water under a pressure gradient through cylindrical pores:

$$\dot{Q}_{H_2O} = -\frac{n\pi r^4 \Delta P}{8\eta \Delta x} \tag{14}$$

in which $\dot{Q}_{H_2O}$ is the volume flow rate of water, n is the number of pores, r is the pore radius, ΔP is the pressure difference, η is the viscosity of water, and Δx is the length of pores, as before. The minus sign indicates that ΔP and

Δx are measured in opposite senses. Since $n\pi r^2 = A_p$, the total pore area, Equation 14 may be written:

$$\dot{M}_{H_2O} = \frac{\dot{Q}_{H_2O}}{\Delta P} = -\frac{r^2}{8\eta}\left(\frac{A_p}{\Delta x}\right) \tag{15}$$

in which $\dot{M}_{H_2O}$ is the volume rate of water flow per unit pressure difference. Combining Equations 13 and 15 to eliminate $A_p/\Delta x$, one obtains an expression for r^2 in terms of known or measurable quantities:

$$r^2 \cong \frac{8\eta \dot{M}_{H_2O} D_{H_2O}}{\dot{m}_{H_2O}} \tag{16}$$

Equation 16 is valid when the pore radius is large in comparison with the radius of the molecule which is diffusing or being filtered through the pore; *i.e.*, when there is no restriction to diffusion or filtration. When the radius of the molecule approaches that of the pore, Equation 16 must be corrected to account for such restrictions. Renkin (31) makes use of two equations which relate equivalent pore area to a function of the ratio a/r, in which a is the radius of the penetrating molecule, and r is the radius of the pore. For restricted diffusion, Renkin's Equation 11 is:

$$\frac{A_{pd}}{A_p} = \left(1 - \frac{a}{r}\right)^2\left[1 - 2.104\left(\frac{a}{r}\right) + 2.09\left(\frac{a}{r}\right)^3 - 0.95\left(\frac{a}{r}\right)^5\right] \tag{17}$$

For restricted filtration, Renkin's Equation 19 is:

$$\frac{A_{pf}}{A_p} = \left[2\left(1 - \frac{a}{r}\right)^2 - \left(1 - \frac{a}{r}\right)^4\right]\left[1 - 2.104\left(\frac{a}{r}\right) + 2.09\left(\frac{a}{r}\right)^3 - 0.95\left(\frac{a}{r}\right)^5\right] \tag{18}$$

In these equations, A_p is the geometrical pore area, A_{pd} is the virtual pore area for diffusion of water, and A_{pf} is the virtual pore area for filtration of water. In the derivation of Equation 16, it was tacitly assumed that $A_{pd} = A_{pf} = A_p$, an assumption valid only in the limiting case when $a/r \to 0$. When a/r is appreciably greater than zero, Equation 16 becomes:

$$r^2 \cong \frac{\dot{M}_{H_2O}\, 8\eta\, D_{H_2O}}{\dot{m}_{H_2O}}\left(\frac{A_{pd}}{A_{pf}}\right) \tag{19}$$

From Equations 17 and 18,

$$\frac{A_{pd}}{A_{pf}} = \frac{1}{2 - \left(1 - \frac{a}{r}\right)^2} \tag{20}$$

Substituting the value of A_{pd}/A_{pf} from Equation 20 in Equation 19 yields:

$$r^2 \cong \frac{\dot{M}_{H_2O}\, 8\eta\, D_{H_2O}}{\dot{m}_{H_2O}\left[2 - \left(1 - \frac{a}{r}\right)^2\right]} \tag{21}$$

Setting $(\dot{M}_{H_2O}\ 8\ \eta D_{H_2O})/\dot{m}_{H_2O} = \lambda$ and rearranging, we have:

$$r \cong -a + \sqrt{2a^2 + \lambda} \tag{22}$$

To find r, we must evaluate λ. At 23°C., $\eta = 9.36 \times 10^{-3}$ poise, and $D_{H_2O}{}^{18} = 2.59 \times 10^{-5}$ cm.²/sec. (by graphical interpolation from the data of Wang *et al.* (13)). $\dot{M}_{H_2O}$ is calculated from the following considerations. There are two components to the total osmotic water flow observed when an osmotic gradient is applied across a membrane. One is caused by diffusion due to the difference in water activity across the membrane; the other, by bulk flow due to this difference (24). Hence, one subtracts the diffusion component from the total osmotic flow to obtain $\dot{M}_{H_2O}$. Thus $\dot{M}_{H_2O} = 0.9 \times 10^{-14}$ ml. H_2O/(sec., cm. H_2O pressure, red cell) $\cong 0.9 \times 10^{-17}$ ml. H_2O/(sec., dynes/cm.², red cell). With these values, $\lambda = 20$ Å². The radius of the water molecule, a, is taken as 1.5 Å (32). Substitution of the values of a and λ in Equation 22 yields $r = 3.5$ Å.

The value of $A_{pd}/\Delta x$ and an estimate of Δx, the membrane thickness, may be used to calculate A_{pd}, the effective pore area for the diffusion of water. However, the estimates of Δx vary from 50 to 5000 Å (33). Let us use these extreme values of Δx to calculate the limiting values of A_{pd}. From the present experiments, $A_{pd}/\Delta x = 3.3 \times 10^{-4}$ cm. For $\Delta x = 50$ Å, $A_{pd} = 1.65 \times 10^{-10}$ cm.², or 0.01 per cent of the total surface area of the human red cell (11). For $\Delta x = 5000$ Å, $A_{pd} = 1$ per cent of the total surface area. Therefore, according to present estimates of membrane thickness, the effective area of pores in the red cell lies between 0.01 per cent and 1 per cent of the total surface. The work of Pappenheimer *et al.* (30) on muscle capillary permeability in the isolated hind limbs of cats provides confirmatory evidence of such small fractional pore areas. They calculated pore areas of less than 0.2 per cent for a molecule the size of water. Further, Parpart and Ballentine (34) have estimated the fractional pore area in rabbit red cells to be 0.1 per cent from a comparison of the free diffusion coefficient of ethylene glycol with its permeability constant in rabbit cells.

Assumptions Involved in Calculation of Equivalent Pore Radius

Several assumptions are involved implicitly in the calculation of equivalent pore radius. Renkin's Equations 11 and 19 are assumed to express correctly the restrictions to diffusion and filtration in 3.5 Å pores. While the equations seem valid for membranes with 15 Å pores on the basis of Renkin's data, their validity at 3.5 Å is conjectural.

The picture of a membrane perforated by uniform, right-cylindrical pores is an idealized geometrical approximation. However, this picture should be regarded as a convenient means of description, rather than as a structural reality, much as is the Stokes-Einstein radius of a molecule. The pore radius calculated above is then an *effective* radius, that is, one which provides a consistent description of the red cell's permeability to water.

The viscosity and diffusion coefficient of water are assumed to have the same values in the 3.5 Å pores as in free solution. Although the diffusion and filtration of water are both probably restricted in a 3.5 Å pore, it is nevertheless assumed in the above treatment that these restrictions can be expressed entirely by changes in $A_p/\Delta x$.

In view of the many uncertainties in the calculation of an equivalent pore radius for a cellular membrane, the result must be viewed with great caution. It is intended to serve as a basis for further experimentation and may be regarded for the moment as an attempt to describe in operational terms a physical property of a complex biological membrane.

BIBLIOGRAPHY

1. Hartridge, H., and Roughton, F. J. W., *Proc. Roy. Soc. London, Series A*, 1923, **104,** 376.
2. Dirken, M. N. J., and Mook, H. W., *J. Physiol.*, 1931, **73,** 349.
3. Chance, B., *J. Franklin Inst.*, 1940, **229,** 455, 613, 737.
4. Solomon, A. K., and Gold, G. L., *J. Gen. Physiol.*, 1955, **38,** 371.
5. Robinson, C. V., *Nucleonics*, 1955, **13,** 90.
6. Coulter, N. A., Jr., and Pappenheimer, J. R., *Am. J. Physiol.*, 1949, **159,** 401.
7. Curran, P. F., private communication.
8. Solomon, A. K., *Advances Biol. and Med. Physics*, 1953, **3,** 65.
9. Roughton, F. J. W., *Proc. Roy. Soc. London, Series B*, 1932, **111,** 1.
10. Wang, J. H., *J. Am. Chem. Soc.*, 1954, **76,** 4763.
11. Ponder, E., Hemolysis and Related Phenomena, New York, Grune and Stratton, Inc., 1948, 14.
12. Sidel, V. W., and Solomon, A. K., *J. Gen. Physiol.*, 1957, **41,** 243.
13. Wang, J. H., Robinson, C. V., and Edelman, I. S., *J. Am. Chem. Soc.*, 1953, **75,** 466.
14. Enns, T., and Chinard, F. P., *Am. J. Physiol.*, 1956, **185,** 133.
15. Graupner, K., and Winter, E. R. S., *J. Chem. Soc.*, 1952, pt. 1, 1145.
16. Løvtrup, S., and Pigón, A., *Compt.-rend. trav. Lab. Carlsberg*, 1951, **28,** série chimique, 1.
17. Johnson, P. A., and Babb, A. L., *Chem. Rev.*, 1956, **56,** 387.
18. Sheppard, C. W., and Martin, W. R., *J. Gen. Physiol.*, 1950, **33,** 703.
19. Ponder, E., Hemolysis and Related Phenomena, New York, Grune and Stratton, Inc., 1948, 120.
20. Beers, Y., Introduction to the Theory of Error, Cambridge, Addison-Wesley, 1953.
21. Roughton, F. J. W., *in* Technique of Organic Chemistry, (A. Weissberger, editor), New York, Interscience Publishers, Inc., 1953, **8,** 669.
22. Jacobs, M. H., *Ann. New York Acad. Sc.*, 1950, **50,** 824.
23. Prescott, D. M., and Mazia, D., *Exp. Cell Research*, 1954, **6,** 117.
24. Durbin, R. P., Frank, H., and Solomon, A. K., *J. Gen. Physiol.*, 1956, **39,** 535.
25. Prescott, D. M., and Zeuthen, E., *Acta Physiol. Scand.*, 1953, **28,** 77.
26. Prescott, D. M., *J. Cell. and Comp. Physiol.*, 1955, **45,** 1.

27. Koefoed-Johnsen, V., and Ussing, H. H., *Acta Physiol. Scand.*, 1953, **28,** 60.
28. Garby, L., and Linderholm, H., *Acta Physiol. Scand.*, 1953, **28,** 336.
29. Ussing, H. H., *in* Ion Transport across Membranes, (H. T. Clarke and D. Nachmansohn, editors), New York, Academic Press, Inc., 1954.
30. Pappenheimer, J. R., Renkin, E. M., and Borrero, L. M., *Am. J. Physiol.*, 1951, **167,** 13.
31. Renkin, E. M., *J. Gen. Physiol.*, 1954, **38,** 225.
32. Morgan, J., and Warren, B. E., *J. Chem. Physic.*, 1938, **6,** 666.
33. Ponder, E., *in* Protoplasmatologia, Handbuch der Protoplasmaforschung, (L. V. Heilbrunn and F. Weber, editors), Wien, Springer-Verlag, 1955, **10,** 2.
34. Parpart, A. K., and Ballentine, R., *in* Modern Trends in Physiology and Biochemistry, (E. S. G. Barron, editor), New York, Academic Press, Inc., 1952.